

Influence of Sintering Temperature on Crystallization Behavior of Cordierite synthesized from Non-Stoichiometric Formulation

K. K. Eing^{1,*}, B. Johar¹, L. N. Ho¹, and Y. Zabari²

¹School of Materials Engineering, University Malaysia Perlis, 02600 Kangar, Perlis, Malaysia

²Advance Materials Department (Ceramic), ADTEC Taiping, 34600 Taiping Perak, Malaysia

Abstract. Cordierite body with formulation of non-stoichiometric composition ($2.5 \text{ MgO} \cdot 1.8 \text{ Al}_2\text{O}_3 \cdot 5 \text{ SiO}_2$) was synthesized using conventional techniques with standard raw materials. The sintering and crystallization behavior of the compositions was observed by Differential Thermal Analysis and Thermogravimetric Analysis (DTA/TG). The sequence of reaction and phase transformation was analyzed using X-ray Diffraction (XRD) technique and Rietveld structural refinement after sintering the samples at different temperature regarding the information from the DTA. The Scanning electron microscopy (SEM) was employed for morphology analysis. The DTA curve shows the crystallization temperature, T_c occur at 1259°C . Rietveld quantitative phase analysis results reveal that α phase Cordierite constitutes up to 96.4 wt% when the samples was sintered for 2 hours at the optimal temperature of 1375°C . The SEM micrograph revealed that the sample was heat treated at 1375°C obtained densified body with well alignment of crystal structure.

1 Introduction

Cordierite (nominal composition $2\text{MgO} \cdot 2\text{Al}_2\text{O}_3 \cdot 5\text{SiO}_2$) know as of the useful crystalline phases in MgO-Al₂O₃-SiO₂ ternary system. Recently, Cordierite has been focuses in numerous important applications due to its excellent properties, such as low thermal expansion coefficient ($3.0 \times 10^{-6}/^\circ\text{C}$), excellent thermal shock resistance, low dielectric constant (4.0-5.0), good chemical durability, excellent refractoriness, and mechanical properties [1-3]. Moreover, cordierite has lower sintering temperature and lower density than the alumina, it also much cheaper and can be synthesized using mineral talc and kaolin [4]. Among the three cordierite polymorph, α -phase is more preference due to it has unique properties, which are very low coefficient of thermal expansion, dielectric constant and dielectric loss, density and stable at elevated temperature [5]. Although α -cordierite is a promising material for many applications, but it is difficult to crystallize and sinter high purity α -cordierite phase at low temperature because of its sintering temperature is near to

* Corresponding author: kuankok29@gmail.com

the incongruent melting point of the cordierite. It has the incongruent melting point because the solid compound of cordierite does not melt to form the liquid of its composition, but instead dissociates to form a new solid phase and the liquid.

Logvinkov et al [6] reported that the change in the crystal lattice of cordierite should be considered as changes arising from composition solid solution rather than phase transformation due to thermodynamic instability of cordierite. Additionally, Torres and Alarcon [7] mentioned that the initial crystalline phase form was cordierite within μ -cobalt and after annealing it transformed to α -cordierite. The μ -cordierite growth along the particle, surface and nucleation and form μ -cordierite dendritic, while the α -cordierite growth within the μ -cordierite dendritic and some Al and Si took place in the tetrahedral sites after long period of annealing at 1100 °C, which introduced some transformation to β -cordierite. Therefore, numerous of studies had been carried out with the purpose of accelerate phase transformation of MgO-Al₂O₃-SiO₂ with cooperation of additive [8-12]. Nevertheless, the TiO₂ was recommended as most effective crystallization catalyst in numerous papers [13-16]. The work of synthesis cordierite through solid state reaction with stoichiometric composition has been carried out by C.Liu et al [17] and founded that, 87 wt% of α -Cordierite formed at optimal sintering temperature of 1350 °C for 3 hours. However, the quantity of α -cordierite observed trending down as elevated the sintering temperature as the result of crystallization of secondary phase such as mullite.

Recently, non-stoichiometric cordierite composition (2.8MgO.1.5Al₂O₃.5SiO₂) has been discovered to give high purity of α -cordierite phase at lower temperature using control crystallization of glass method [4]. The present of high concentration of secondary phase such as forsterite, spinel and mullite (which have different coefficient of thermal expansion and different volume) in cordierite synthesis using stoichiometric composition might affect the performance and its application especially in evaluated temperature atmosphere. The Cordierite body synthesized through glass method by using non-stoichiometric cordierite formulation 2.8MgO.1.5Al₂O₃. 5SiO₂ obtaining single phase α -phase Cordierite (100 wt%). However, in previous work, the cordierite with same formulation has been synthesized by solid state reaction and more than 10 wt% of secondary phase such as enstatite was observed. The formation of secondary phase was mainly contributed by excess of MgO in the system. Hence, in this present study, the Cordierite body has been synthesized through solid state reaction by alternated the mole ratio of MgO and Al₂O₃ to 2.5MgO. 1.8Al₂O₃. 5SiO₂ in order to obtain high purity (>95%) stable α - cordierite.

2 Materials and method

α -Cordierite with non- stoichiometric formulation was synthesized using reagent grade oxides (MgO, Al₂O₃, and SiO₂) with 5 wt% of TiO₂ as nucleating catalyst. The magnesia was obtained for R&M Marketing, Essex, U.K, Alumina and silica were obtained from MajuSaintifikSdn.Bhd. Table 1 showed the elemental analysis of the raw materials, while Table 2 gives the details on weight percent of the non-stoichimetric cordierite formulation composition in this study. The particle size of the reagent oxide was sieved and determined by using particle size analyzer to ensure the median of the particle size d_{50} less than 30 μ m. The components were weighted and mixed thoroughly by using jar mill together with 10 mm diameter alumina balls as media at rotation speed of 136 RPM for 36 hours. The batchers were compacted at 7 tones into pellet form of 20 mm in diameter by using hydraulic powder press (CARVER AUTO 3890). The green body compact were sintered at different temperature, which were 1250°C, 1275 °C, 1300 °C, 1325°C, 1350°C and 1375 °C for 2 hours at a heating rate of 10 °C/min respectively

The qualitative and quantitative crystalline phases of specimens were characterized by using X-Ray diffraction (XRD) (RigakuUltimaIV) with Cu K α radiation, in the $5^\circ \leq 2\theta \leq$

90° range at a scanning rate of 1 °/min. Crystal structure analysis was carried out with whole diffraction powder pattern data by utilized Rietveld Refinement method using XpertHighScore Plus software. Differential Thermal Analysis and Thermogravimetric Analysis (DTA/TG) (Rigaku TG 8120) technique was employing to identify the thermal behavior of the batch. The thermal analysis was made in range 40-1500 °C by using corundum crucible as an inert reference material at heating rate of 10 °C /min. The Microstructure of the sintered samples was observed by scanning electron microscopy, SEM (Hitachi TM3000).

Table 1. Elemental analysis reagent oxides compound by XRF.

	Chemical Composition (wt%)												
	MgO	Al ₂ O ₃	SiO ₂	P ₂ O ₅	K ₂ O	CaO	Fe ₂ O ₃	NiO	ZnO	Ga ₂ O ₃	SO ₃	Cl	Na ₂ O
Al ₂ O ₃	-	99.50	0.17	-	0.03	0.05	0.05	0.02	0.01	0.02	-	-	0.16
MgO	95.10	0.72	0.71	0.10	-	1.11	0.08	-	-	-	1.96	0.22	-
SiO ₂	0.06	0.88	98.40	0.04	-	0.30	0.06	0.02	-	-	-	-	0.08

Table 2. Composition (wt%) of initial raw materials with formulation 2.5MgO.1.8Al₂O₃. 5SiO₂.

Sample	Wt %			
	MgO	Al ₂ O ₃	SiO ₂	TiO ₂
2.5MgO.1.8Al ₂ O ₃ . 5SiO ₂	18.09	35.81	50.42	5.216

3 Results and discussion

3.1 Crystallization behavior

Differential Thermal Analysis and Thermogravimetric Analysis (DTA/TG) curves recorded on the thermal behaviour of the non-stoichiometric cordierite composition of 2.5Mg.1.8Al₂O₃.5SiO₂ from 40 to 1500 °C are shown in Figure 1. As can be seen in Figure 1, the thermogravimetric (TG) curve of the sample has been segregated into 7 regions. The regions A to F was corresponding to the mass losses, while there was mass gain occur at region G which is related to the crystallization and phase transformation. At the first region, the initial weight losses about 0.73% occurs in the range between 40 and 190 °C which is corresponding to the elimination of water physically adsorbed when wet method mixing route was carried out. Followed by the major weight change about 3.61% losses in the temperature range of 190 to 388 °C, which can attributed to the dehydration of the MgO. The existence of endothermic peak in DTA plot at 588 °C further supports the observation. The mass losses about 1.84% and 1.17% was observed in temperature range 388 to 447 °C (region C) and temperature range 447 to 569°C (region D) respectively. The mass losses occur in region C is contributed by the decomposition or organic burn out of the sample. While in region D, the small endothermic peak was observed at 564 °C, which is correlated to the phase transformation of silica. There is no significantly weight change in region E. However, the transition temperature, T_g endothermic peak of the sample was presence at 772 °C in the DTA curve at this particular peak.

The exothermic peak of was detected at 979 °C and reaching at endothermic at 1163 °C in the DTA curve and about 0.14% weight losses in region F . In this region the nucleation of glass might take place due to the nucleation temperature (T_n), is usually taken in the nucleation range, which is between T_g and softening point (T_d) [18] and it can be calculated by using formulation:

$$T_n = T_g + 2/3 (T_d - T_g) \quad (1)$$

Considering the endothermic peak at 1163 °C is softening point of the samples, thus the nucleation temperature, T_n of sample was located at 1132.67 °C. A shape exothermic crystallization peak was presence at 1259 °C, which is corresponding to the phase transformation of μ -Cordierite to α -Cordierite [19]. Moreover, thermogravimetric curve in region G shown mass gain causes by solid state reaction of decomposition and leading formation of α -Cordierite and leading the variation of samples density of the sample. The sequence of reaction and phase transformation occurs in region G was detailed by the X-ray Diffraction (XRD) pattern.

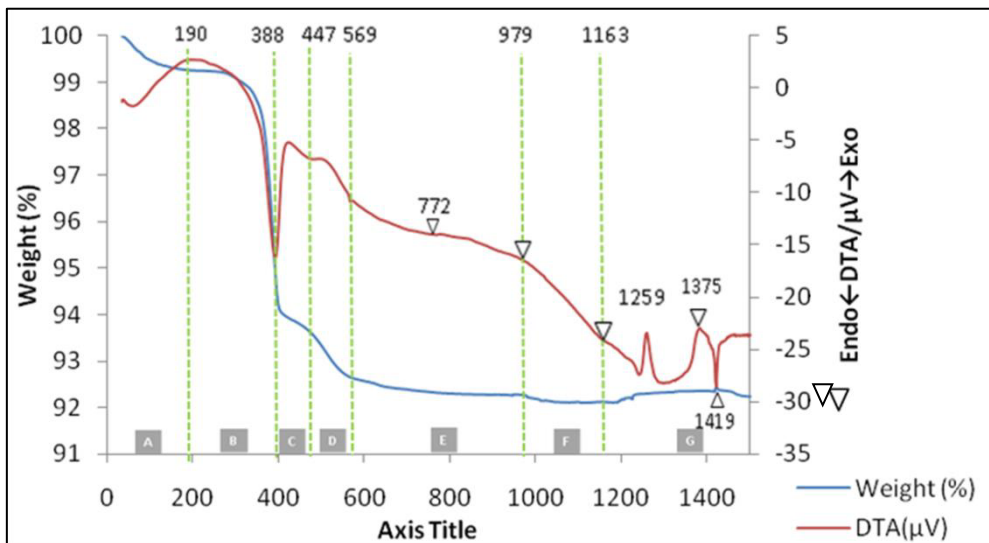


Fig. 1. DTA/TG curve for composition of 2.5MgO. 1.8Al₂O₃. 5SiO₂.

3.2 Phase evolution

To investigate the sequence of reactions and phase transformation, the samples were heat-treated at different temperatures. According to crystallization temperature, T_c , and information of Figure 1, the samples heat treated at 1250 °C, 1275 °C, 1300 °C, 1325 °C, 1350 °C and 1375 °C. Figure 2 and Figure 3 present the phase identification of XRD patterns and Rietveld quantitative phase analysis of the samples with non-stoichiometric cordierite formulation of 2.5Mg.1.8Al₂O₃.5SiO₂ sintered at different temperature for 2 hours as dwell time respectively. The result indicate that, the thermal treating heat have greatly impact on the purity of α -Cordierite. The α -Cordierite (ICSD # 98-004-5314) peak was observed in the entire XRD pattern, and the intensities of the corresponding peaks increases with increasing temperatures of 1250 °C-1375°C. Rietveld quantitative phase analysis results reveal that α -Cordierite constitutes up to 96.4 wt% of the samples sintered for 2 hours at the optimal temperature of 1375 °C. At 1250°C, the α -Cordierite was the

dominant phase. However, the secondary phase such as Sapphirine (ICSD# 98-007-8446), Cristobalite low (ICSD# 98-001-6962), Quartz (ICSD# 98-003-5149), spinel (ICSD# 98-005-8347) and Rutile (ICSD# 98-007-6756) was observed. Furthermore, about 6.3 wt% of μ -Cordierite (ICSD# 98-010-9832) was presence at sintering temperature 1250°C due to the the uncompleted phase transformation which is related to result obtained from DTA curve in Figure 1. Further raise up the sintering temperature to 1275 °C, the completely phase transformation leads to increased amount of α -Cordierite from 52.3 wt% to 59.4 wt%. Additionally, the Magnesium Dtitanate (ICSD# 98-005-3931) was observed as decomposed of Rutile. Alongside, the disintegration of minor phase such as quartz high and Cristobalite high might prop up the amount of Sapphirine. This phenomenon also can be seen in sintering temperature 1300 °C, the amount of α -Cordierite and Sapphirine increased as further decomposition of quartz and Cristobalite. Meaning that, the decomposition of quartz or Cristobalite contributed Si^{2+} and O^- in the mixed system and it might endorse the formation of α -Cordierite and Sapphirine at particular sintering temperature. As increase of the sintering temperature form 1300 °C to 1325 °C, it could be noticed the amount of Sapphirine is decrease and the Spinel peak was detected. The Sapphirine was totally vanished at 1350 °C and left behind the small amount of Spinel. Moreover, crystalline content of α -Cordierite phase has dramatically intensified to 90 wt% as disintegration of Sapphirine. The crystalline phase content of α -Cordierite was achieved up to 96.7 wt% as decomposition of Spinel at sintering temperature of 1375 °C for 2 hours soaking time with minor secondary phase of Anosovite (Ti_3O_5) (ICSD# 98-001-1581) and Aluminium Magnesium ($\text{Al}_{0.9}\text{Mg}_{0.9}$) (ICSD# 98-006-5874). This is competitive result with stoichiometric cordierite formulation [17] [20]

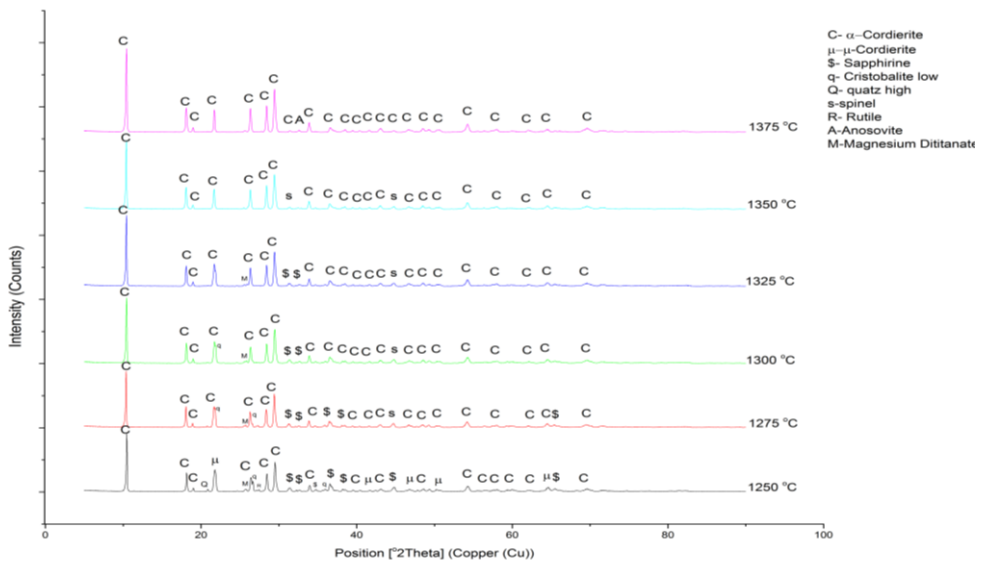


Fig. 2. XRD patterns of samples sintered at temperature ranging from 1250 to 1375 °C for soaking times of 2 hours.

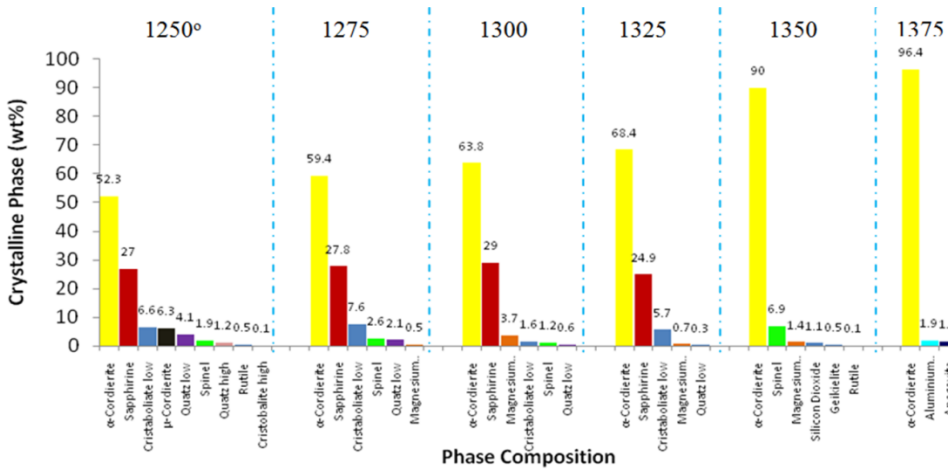


Fig. 3. Crystalline phase content of samples sintered at temperature ranging from 1250 to 1375 °C for soaking times of 2 hours.

3.3 Microstructure analysis

Figure 4 illustrated the Scanning electron microscopy (SEM) images of the samples heat treated at different temperature for 2 hours. It was found that, the sample has heat treated at 1375 °C (Figure 4f) obtained optimal morphology and fined microstructure as well as α -Cordierite hexagonal crystal structure was formed over the surface of the sample. Conversely, the formation of secondary phase induce the rough morphology as can be seen in Figure 4a. With corroborating the results obtained through XRD, in can be noticed that, the morphology of samples show better appearance more denser body as diminish of secondary phase

Figure 5, showed the comparison between the samples sintered at 1250 °C and 1375 °C. As can be seen in Figure 5a, the formation of dissimilar and complex crystal structure of secondary phase has inferior alignment with other phase and induce pore between each other. As a result, the performance in terms of mechanical strength, thermal expansion coefficient, and dielectric constant has impacted. On the other hand, the approximately single phase of α -Cordierite present well alignment of the crystal structure.

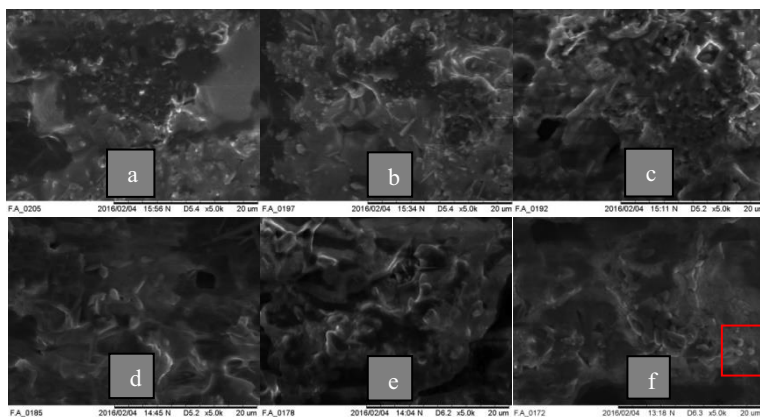


Fig. 4. SEM micrograph of samples sintering at (a) 1250 °C, (b) 1275 °C, (c) 1300 °C, (d) 1325 °C, (e) 1350 °C, (f) 1375 °C for 2 hours under magnification of 5000X.

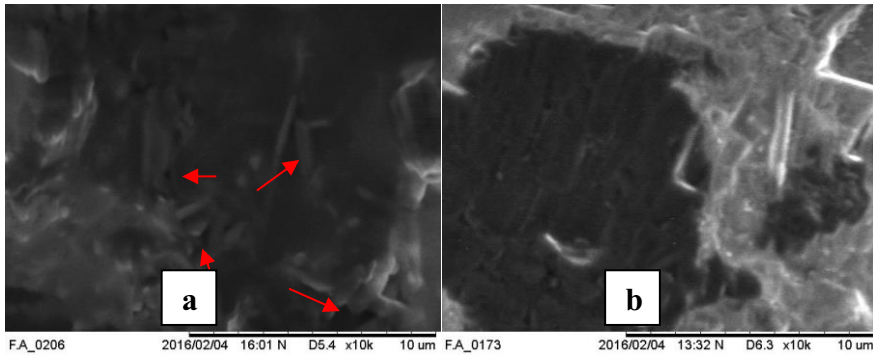


Fig. 5. The SEM micrograph of samples sintering at (a) 1250 °C, (b) 1375 °C for 2 hours under magnification of 10000X.

4 Conclusions

The high purity of α phase Cordierite has been successfully synthesized from non-stoichiometric formulation $2.5\text{MgO} \cdot 1.8\text{Al}_2\text{O}_3 \cdot 5\text{SiO}_2$ using a conventional technique with standard raw materials. The X-ray diffraction technique and the Rietveld quantitative phase analysis results reveal that α -Cordierite constitutes up to 96.4 wt% of the samples sintered for 2 hours at the optimal temperature of 1375 °C. With corroborating of XRD patterns and DTA curve, the μ -Cordierite has been confirm completely transformed to α -Cordierite at sintering 1275 °C. SEM micrograph revealed that fully dense with well crystal structure alignment α -Cordierite was successfully crystallized.

The authors gratefully acknowledge the financial support from the fundamental Research Grant Scheme (FRGS 900300495) Universiti Malaysia Perlis and equipments support from ADTEC Taiping Malaysia.

References

1. X. Guo, N. Kazuki, K. Kazuyoshi, Y. Zhu, H. Yang, J. Eur. Ceram. Soc., **34**, 817 (2014)
2. P. Orosco, M. del C. Ruiz, J. Gonzalez, Powder Technol., **267**, 111 (2014)
3. Y. Dong, X. Liu, Q. Ma, G. Meng, J. Memb. Sci., **285**, 173 (2006)
4. J. Banjuraizah, M. Hasmaliza, Z.A Arifin, J. Alloys Compd., **482**, 429 (2009)
5. J. Banjuraizah, H. Mohamad, Z.A Ahmad, J. Alloys Compd., **509**, 7645 (2011)
6. S. M. Logvinkov, G. D. Semchenko, D. A. Kobyzeva, V. I. Babushkin, Refractories and Industrial Ceramics, **42**, 434 (2001)
7. F. J. Torres, J. Alarcon, J. Eur. Ceram. Soc., **24**, 681 (2004)
8. Z. Yuea, J. Zhoua, Z. Maa, J. Baoa, Z. Guia, L. Lia, Ferroelectrics, **262**, 31 (2001)
9. X. Hao, Z. Luo, X. Hu, J. Song, Y. Tang, A. Lu, Journal of Non-Crystalline Solids **432**, 265 (2016)
10. L. Barbieri, C. Leonelli, T. Manfredini, R. Bertocello, Journal of Materials Science, **29**, 6273 (1994)
11. C. Leonelli, T. Manfredini, M. Paganelli, P. Pozzi, G.C. Pellacani, Journal of Materials Science, **26**, 5041 (1991)

12. H.S. Kim, R.D. Rawlings, P.S. Rogers, *Journal of Materials Science*, **24**, 1025 (1989)
13. M. Rezvani, B.E. Yekta, V.K. Marghussian, *J. Eur. Ceram. Soc.*, **25**, 1525 (2005)
14. J. Yang, S.G. Zhang, B. Liu, D.A. Pan, C.L. Wu, A.A. Volinsky, *Journal of Iron and Steel Research*, **22**, 1113 (2015)
15. M. Fathia, A. Johnson, *Dental Materials*, **32**, 311 (2016)
16. K. Maeda, Y. Sera, A. Yasumori, *Journal of Non-Crystalline Solids*, **434**, 13 (2016)
17. C. Liu, L. Liua, K. Tan, L. Zhang, K. Tang, X. Shi, *Ceramics International*, **42**, 734 (2016)
18. V. I. Marghussian, M. H. D. Niaki, *J. Eur. Ceram. Soc.*, **15**, 343 (1995)
19. LingHong, H. Zhou, C. Xu, *Journal of Materials Science* **13**, 381 (2002)
20. N. Obradovic, N. Dordevic, S. Filipovic, N. Nikolic, D. Kosanovic, M. Mitric, Markovic, V. Pavlovic, *Powder Technol.*, **218**, 157 (2012)